The Correlation between GOES Flare Classification and the Impact of Solar Flaring on Geomagnetic Field Strength

Kevin Beach

Chippewa Hills High School

December 29, 2011

Abstract

The solar wind can affect Earth's magnetic field. The Geostationary Operational Environment Satellites (GOES) classification system classifies flares based on their X-ray flux. This study investigated a possible correlation between the GOES classifications of solar flares and changes in the strength of the Earth's magnetic field. Data were downloaded for the Bz component of the Interplanetary Magnetic Field (IMF) position and speed (km/sec) on flare dates between 2006 and 2011 using Advanced Composition Explorer (ACE) data archives. Geomagnetic field data were also downloaded from THEMIS data archives for the days possibly affected by the solar flares. The time when high-energy particles from each solar flare reached Earth was determined using ACE data. This arrival time was used in the magnetic field data to focus in on the time when the Earth's magnetic field was first affected by the flare. The variations of the geomagnetic field's strength were shown by creating a scale that measures the intensity of geomagnetic disturbances. The GOES classifications and scale values were than graphed together in scatter plots where R^2 values of 0.2391, 0.1638, 0.0464, and 0.0862 were found. These R^2 values indicated that there was a weak correlation between GOES classifications and B_z component variations. Histograms were also constructed to further illustrate the data. The separation of data points in the histograms further supports the conclusion.

Acknowledgements

I would like to acknowledge the help of a few individuals over the course of this research. Mr. Cris DeWolf, my research mentor, was a great help to me assisting with locating resources as well as the editing of my paper, board, and presentation. Dr. Leif Svalgaard, whom I met through the internet, was a great help to me with editing my data analysis and furthering the process of editing my paper for presentation. John Day, an ex-Air Force pilot, was of great help to me in his assistance by helping me further explain the Geomagnetic Variational Intensity Scale. Devon VanOrder, a good friend, was able to help me throughout the project in merely listening to my explanation of the project as I progressed to be able to tell me if it was understandable to the average student. Alex Conati, another friend, helped me in the beginning of the project and obtained ACE data for the year of 2008.

Table of Contents

List of Figures

List of Tables

List of Graphs

Introduction

Solar flares are sudden outbursts of energy from the Sun, in fact the biggest explosions in the Solar System. It is thought that they originate in the corona of the Sun, where temperatures are the hottest. Solar flares are created during magnetic reconnection of the magnetosphere on the sun in areas where the field has undergone fluctuations. (Demoulin, van Driel-Gesztelyi, Schmieder, Henoux, Csepura, & Hagyard, 1992) These fluctuations open up weak points in the magnetosphere where the enormous amount of energy escapes. Solar flares mainly comprise energy in the form of high frequency X-rays, ultraviolet radiation, and large amounts of light. Because of this, it is rare that a flare is strong enough to show against the white light spectrum of the Sun, meaning flares most often must be observed through high frequency specific instruments. The radiation from intense solar flares can reach the Earth in as little as 499 seconds. Along with this radiation, extremely energized particles can take, at times, less than an hour to reach Earth. These particles can be very influential not only on the Earth's atmosphere and magnetic field but can destroy satellite electronics and noticeably affect our own electrical grid. (Lang, 2006)

Earth's magnetic field has a dipolar structure such as if there was a bar magnet in the core of the Earth. The axis of the dipole is tilted 11 ½° from the Earth's rotational axis. Due to this, the north and south magnetic poles and geographic poles are in different locations. (Weigel, 2005) This field is split into three components. The components are the B_x directed to the north, B_y directed to the east, and B_z directed positive downwards. These components of the magnetic field are considered vectors in the sense that when you take the square root of their squared sum, you get the total B field. To demonstrate: $B_{tot}=\sqrt{B_x^2+B_y^2+B_z^2}$. The average measurement of the total B field is close to 50,000 nanoTeslas. (Pedersen, 2001)

The most commonly used scale to classify solar flares is the NOAA GOES scale. It measures X-ray brightness of flares in the wavelength range of one to eight Angstroms. The measurements are then put onto a scale which classify flares in an ascending order of A, B, C, M, and X. On each letter of the scale, there are 9 divisions such as M1, M2, M3… and M9. Decimal numbers following the first digit are common for more precise measurement. C flares occur most frequently of the C, M, and X level flares and pose nearly no threat to any Earth-based or Earth-orbiting systems. M and X flares occur not nearly as frequently, but pose a larger threat and cause radio blackouts and radiation storms varying in strength. ("The classification of,")

The goal of this study was to find evidence to help support or discredit the idea that the GOES classification of solar flares can be correlated to the strength of the B_z component of the geomagnetic field. This was achieved by looking at the strength of B_z in response to impacting solar flares. Data for the project were collected from three separate sources. The first source was the ACE spacecraft level 3 data archive which was used for solar wind speed, solar wind density, and IMF position data. The second source was the THEMIS (Time History of Events and Macroscale Interactions During

Substorms) data archive for the ground-based magnetometer in Remus, MI, which was used for the strength of the B_z component of the Earth's magnetic field. The last source was the NOAA SWPC (Space Weather Prediction Center) archive which handles data on the GOES classifications of solar flares along with the time at which they occurred from the GOES 15 spacecraft's measurements.

In order to measure the potential impact of solar flares on the geomagnetic field, a new data reduction system was created. This system was called the GVIS (Geomagnetic Variational Intensity Scale). The GVIS was created to evenly and accurately measure the intensity of geomagnetic variations caused by solar flares. The calculations result in a scale which is able to show a level of variation in the strength of the magnetic field at the time which the number is calculated for.

The ACE mission was originally proposed in 1986 as a part of the Explorer Concept Study Program to take coordinated measurements of the elemental and isotopic composition of accelerated nuclei in solar phenomena. It was selected for development in 1989 and construction began on it in 1994. ACE was launched on August 25, 1997 from Cape Canaveral Air Station on a Delta II rocket. Its scientific goals include studying the composition of distinct samples of matter such as the solar corona, interplanetary medium, local interstellar medium, and galactic matter. The way it will accomplish this is by studying the composition of the solar wind, coronal mass ejections, and the solar energetic particles in solar flares. The data it collects consists of the strength of the IMF (Interplanetary Magnetic Field), solar wind velocity, and the density of particles in the solar wind. (Stone, Frandsen, Mewaldt, Christian, Margolies, et al, 1998)

The THEMIS (Time History of Events and Macroscale Interactions During Substorms) mission was originally started to study the magnetotail and the sequence of events that cause auroral substorms in the atmosphere. Auroras are caused by charged electrons in the atmosphere from the enhanced solar winds. The electrons travel along magnetic field lines and interact with gases in the atmosphere which causes the gases to heat up and emit light ("Sun-earth connection," 2011). In order to find out the order of events which cause the substorms, a group of five identically-instrumented spacecraft was sent into space where each align once every four days over the array of ground observatories which are located in the Northern USA and Canada ("Themis overview" 2011). Eleven magnetometers were installed in schools across the US as part of the THEMIS public outreach program. The magnetometers measure the strength of the magnetic field across time at two measurements per second (Russell, Chi, Dearborn, Ge, Kuo-Tiong, et al, 2008). The data from the Remus, MI ground-based magnetometer was used in this study for comparison to the ACE data at corresponding times.

The NOAA SWPC (Space Weather Prediction Center) is part of the National Weather Service. The SPWC uses data from GOES (Geostationary Operational Environmental Satellites) to measure x-ray flux of solar flares and provide data of when they occur (NWS internet services team, 2008). The satellites are part of the NOAA's mission to gain knowledge on the Earth's weather patterns. They provide continuous monitoring of the Earth in a geosynchronous orbit above the equatorial plane of the Earth with a speed matching Earth's rotation. This means they will hover over one spot on the Earth from 35, 800 km away ("NOAA's geostationary and," 2010). Attached to GOES 12 through 15 are sophisticated solar X-ray Imagers that monitor the Sun's X-rays to detect solar flares, CMEs, and other events which impact the geospace environment. The data from the X-ray Imager aboard GOES 15 was used to find the dates and time of day which solar events occurred ("Goes solar x-ray," 2010).

Materials

To obtain the data for this study many different websites linked to scientific missions in space were used. Each was created independently for different purposes. The NOAA SWPC event summary archive provided recent data from solar and geomagnetic indices and solar event reports that were created from preliminary reports ("Space weather prediction," 2011). Archived daily report files were used from the website to locate indices of when M and X class solar flares (on the GOES solar flare classification scale) were created by the sun. The ACE (Advanced Composition Explorer) level 3, unverified but contributed, data browser was used to obtain data on specific flares. The ACE mission has nine different instruments on the satellite which is in orbit around the Earth 1/100th the distance away from the Earth to the Sun. Two of the nine instruments on the ACE satellite were used; these included the SWEPAM and the MAG. SWEPAM (Solar Wind Electron Proton & Alpha Monitor) measures ionic particle energies between .26-36 KeV and electron charges between 1-1350 eV. It also measures the particle density of solar winds in particles/cm^3 and the speed of solar winds in Km/sec ("Swepam solar wind," 2011). MAG (Magnetometer) measures the IMF (Interplanetary Magnetic Field) direction and magnitude that was used in this study (Smith, 2011). The THEMIS (Time History of Events and Macroscale Interactions During Substorms) data browser was used to obtain geomagnetic data from the Remus, MI, ground station. This data archive is constantly receiving data from this magnetometer, supplied to Chippewa Hills High School in Remus, Michigan as part of the THEMIS mission education and public outreach effort. The magnetometer measures the strength of the magnetic field constantly and the Bx, By, and Bz components separately. It was used to obtain the data which was examined for any potential impact of a solar flare's energized particles on the Bz component of the magnetosphere in the localized region of Remus, Michigan. (Russell, Chi, Dearborn, Ge, Kuo-Tiong, et al, 2008)

Methods

For data from the SWPC archive site, the days were searched starting from August 11 to as far back as 2006 to obtain enough dates of solar flares that could be used for this study. The date, time, and GOES class were all recorded in a separate Microsoft Word file for easy access later on. Any solar flares within two hours of each other were then removed from the list due to a lack of specificity in the THEMIS and ACE data later on. After the flare data were obtained matching THEMIS data were downloaded. In order to obtain the THEMIS data, the browser was used and selected to access data from Remus, Michigan. The data for two to four days after the solar flare initially left the Sun was collected as a text file for every grouping of thirty to seventy-two hours after each solar flare. Once this data was collected, an Excel spreadsheet was set up where the raw data was placed on Sheet 2 and the formulas and results on Sheet 1. Formulas were written to find the mean, median, and mode of each hour of the day of the magnetic field Z component data so there were 24 means, medians, and modes. Another spreadsheet was made for five-minute averages of the THEMIS data with each hour of the day in a separate sheet on the document. It calculated the mean, median, and mode of every five minutes of each hour of the day of the magnetic field's Z component data so there were 288 means, medians, and modes. The data were replaced for each day of the THEMIS data in the spreadsheet by using the Refresh All button under the Data tab. Once all the formulas had re-calculated it was saved using Save as so as to preserve the main file to save time. The last spreadsheet used was a simple one-sheet spreadsheet that had a line graph of each day's magnetic field readings by the bi-second measurements shown. Then, the ACE data for the same time frame (two to four days) after the initial release of the solar flares was downloaded from the ACE level 3 data browser and put into text files where the data could be accessed. In order to find the arrival of the solar flares the hourly ACE data was examined for a spike in the speed and density of the solar wind. When the spike was located the five-minute average data was examined to pinpoint a more accurate arrival time of the solar flare at the ACE satellite. On average, it would take between two to five hours for energetic flare particles to travel from ACE to Earth. Magnetometer data for this time frame was examined, looking for where the flare particles started to affect the magnetic field. When the hour at which the effect of the solar flare was most evident was determined, the five-minute average data was used to establish a more accurate reading of the magnetic field's strength during the time frame of any potential impact by energetic flare particles. The maximum magnetic field strength upon the arrival of each flare was extracted from the full day spreadsheet and was represented by the variable 'M'. Then the point at which the magnetic field had changed the most, represented by the variable 'N', to the point where the magnetic field had most nearly recovered from the blast, represented by the variable 'P', was averaged, then the average of all points between 'N' and 'P' was assigned the variable 'D'. 'A' was the result of dividing the maximum 'M' by the variable 'D'. The time, in seconds, was represented by 'T'. The formula for calculating the GVIS using the variables was $GVIS = \log(\frac{A}{T})$, when A > 1; $GVIS = \log(\frac{T}{A})$, when A < 1; and $GVIS = 0$, when A =1. When A > 1, a weakening of the field was indicated by the result of $GVIS = \log(\frac{A}{T})$, and when A < 1, a strengthening of the field was indicated by the result of $GVIS = \log(\frac{T}{A})$. When A = 0, $GVIS = 0$ indicated no change in the field's strength. These numbers were then taken and graphed on a scatter plot in Excel against the GOES classifications of each flare. An R-squared value was generated for the plot to evaluate any correlation between the GVIS and GOES classification. Histograms of the GVIS values and GOES classification showing the distribution of GOES classified flares among the GVIS values were generated to more graphically illustrate the results.

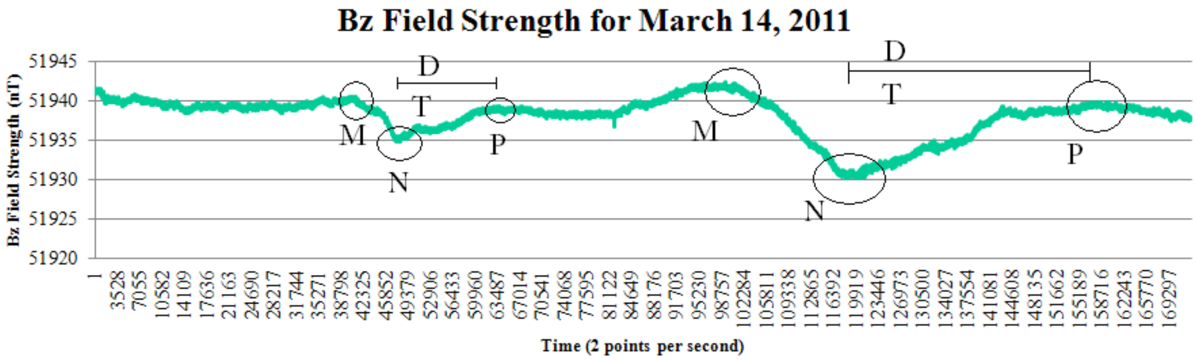

Figure 1

Results

Table 1

Date of Solar Flare	GOES Classification of Flare	Peak X-ray Flux between 1 and 8 Angstroms	GVIS Value of Flare
November 15, 2011	M1.1	1.1e-5	3.813727573
November 9, 2011	M1.1	1.1e-5	4.492359886
November 6, 2011	M1.2	1.2e-5	-4.22315723
November 5, 2011	M1.8	1.8e-5	3.810593785
November 5, 2011	M1.1	1.1e-5	3.723682829
November 5, 2011	M3.7	3.7e-5	-3.81043103
November 4, 2011	M1.0	1.0e-5	-3.09566786
October 22, 2011	M1.3	1.3e-5	4.511238455
October 2, 2011	M1.3	1.3e-5	-4.1420192
October 2, 2011	M3.9	3.9e-5	3.656775164
October 1, 2011	M1.2	1.2e-5	-3.29643681
September 30, 2011	M1.0	1.0e-5	-3.87491345
September 28, 2011	M1.2	1.2e-5	3.895696911
September 26, 2011	M2.6	2.6e-5	-3.62275752
September 26, 2011	M4.0	4.0e-5	-3.43885452
September 10, 2011	M1.1	1.1e-5	-3.7828025
September 9, 2011	M1.2	1.2e-5	-3.29124582
September 9, 2011	M2.7	2.7e-5	-3.61352371
September 8, 2011	M6.7	6.7e-5	-4.40518277
September 7, 2011	X1.8	1.8e-4	3.779890746
September 6, 2011	X2.1	2.1e-4	-4.29709013
September 6, 2011	M5.3	5.3e-5	-3.99279109
September 4, 2011	M3.2	3.2e-5	-3.72864691
August 9, 2011	X6.9	6.9e-4	4.166263611
August 9, 2011	M2.5	2.5e-5	-3.751679801
August 8, 2011	M3.5	3.5e-5	-3.443620046
August 4, 2011	M9.3	9.3e-5	-3.815927097
August 2, 2011	M1.4	1.4e-5	-3.326300602
June 14, 2011	M1.3	1.3e-5	-4.112979280
May 29, 2011	M1.4	1.4e-5	4.359456760
May 28, 2011	M1.1	1.1e-5	-3.755484060
April 22, 2011	M1.2	1.2e-5	-2.899730612
April 22, 2011	M1.8	1.8e-5	-3.041366249
March 25, 2011	M1.0	1.0e-5	-4.097308398
March 23, 2011	M1.4	1.4e-5	-3.449076036
March 15, 2011	M1.0	1.0e-5	4.122548913
March 12, 2011	M1.3	1.3e-5	-4.021061014
March 10, 2011	M1.1	1.1e-5	-3.214708110
March 8, 2011	M5.3	5.3e-5	-3.480286481
February 18, 2011	M1.3	1.3e-5	-3.928183557
February 15, 2011	X2.2	2.2e-4	-4.112676318
February 13, 2011	M6.6	6.6e-5	-3.800096959
June 13, 2010	M1.0	1.0e-5	-4.191078272

Date of Solar Flare	GOES Classification of Flare	Peak X-Ray Flux between 1 and 8 Angstroms	GVIS Value of Flare
June 12, 2010	M2.0	2.0e-5	-4.325899590
February 12, 2010	M1.1	1.1e-5	-3.233578102
February 12, 2010	M8.3	8.3e-5	3.972414336
January 20, 2010	M3.4	3.4e-5	-4.014115866
January 20, 2010	M1.8	1.8e-5	3.951862740
March 25, 2008	M1.7	1.7e-5	4.114026014
June 9, 2007	M1.0	1.0e-5	-3.323037126
June 4, 2007	M8.9	8.9e-5	-4.099731714
June 3, 2007	M4.5	4.5e-5	-3.961182916
June 2, 2007	M1.0	1.0e-5	-3.494772199
June 2, 2007	M2.5	2.5e-5	-3.576896425
June 1, 2007	M2.1	2.1e-5	3.930035309
June 1, 2007	M2.8	2.8e-5	-3.394009052
June 1, 2007	M1.0	1.0e-5	-3.761974518
December 14, 2006	X1.5	1.5e-4	-4.467556739
December 13, 2006	X3.4	3.4e-4	4.457632687
December 6, 2006	M6.0	6.0e-5	-3.306721454
December 6, 2006	M1.1	1.1e-5	-3.228348013
July 6, 2006	M2.5	2.5e-5	-3.588653874
April 27, 2006	M7.9	7.9e-5	-3.936462030
April 26, 2006	M1.3	1.3e-5	3.909758396

Graph 1

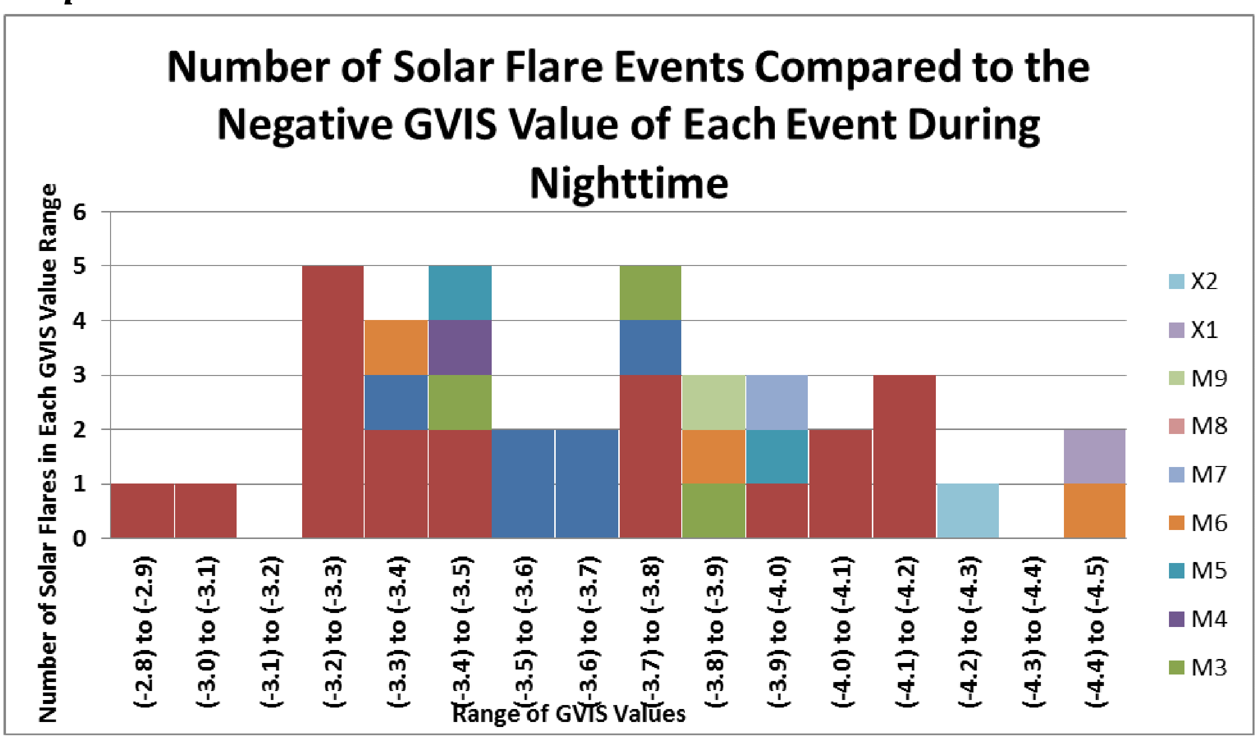

Graph 2

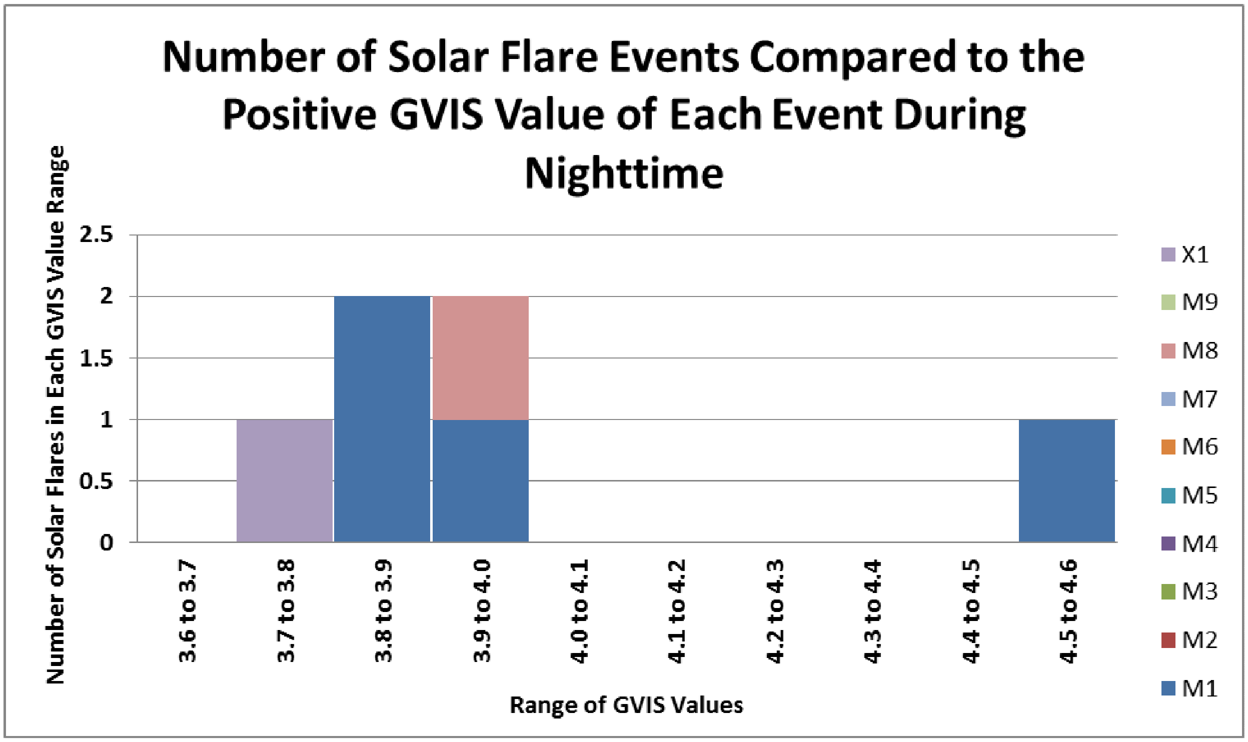

Graph 3

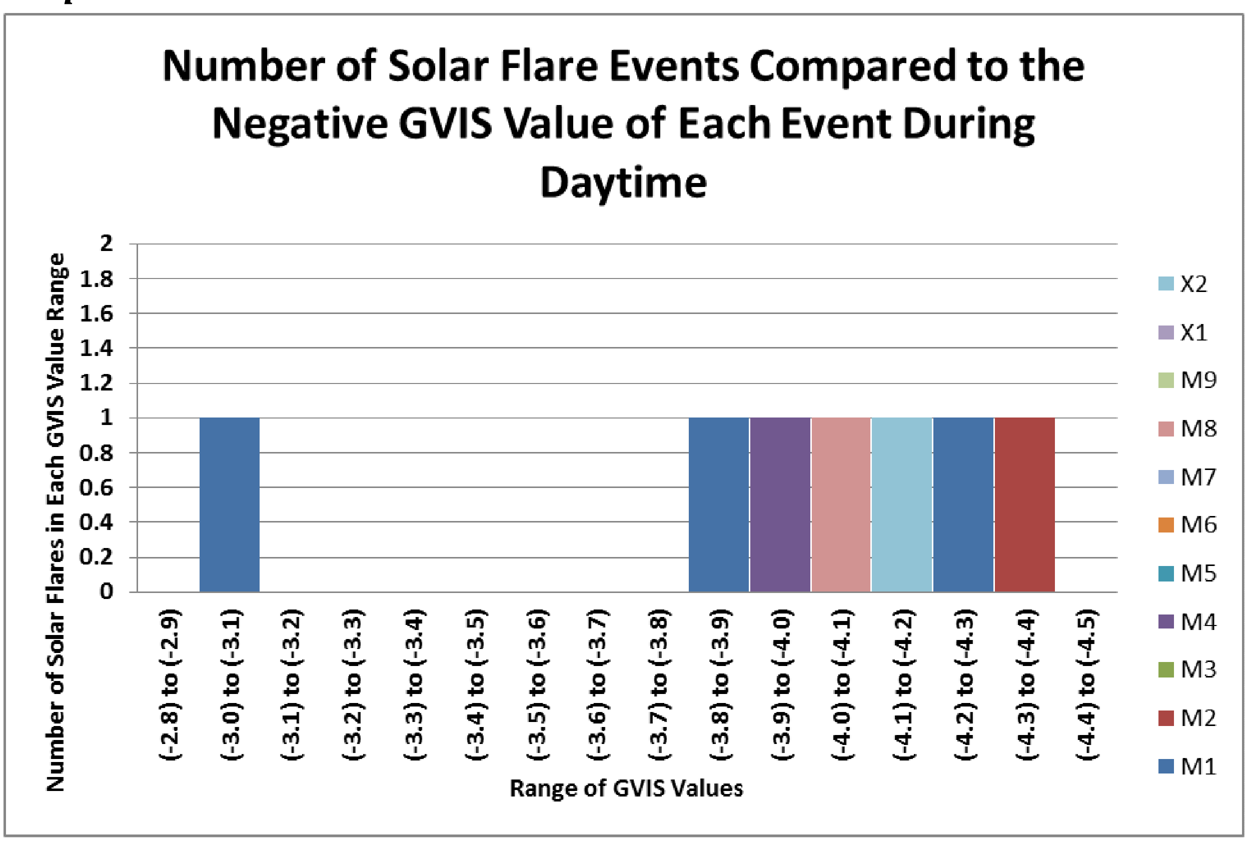

Graph 4

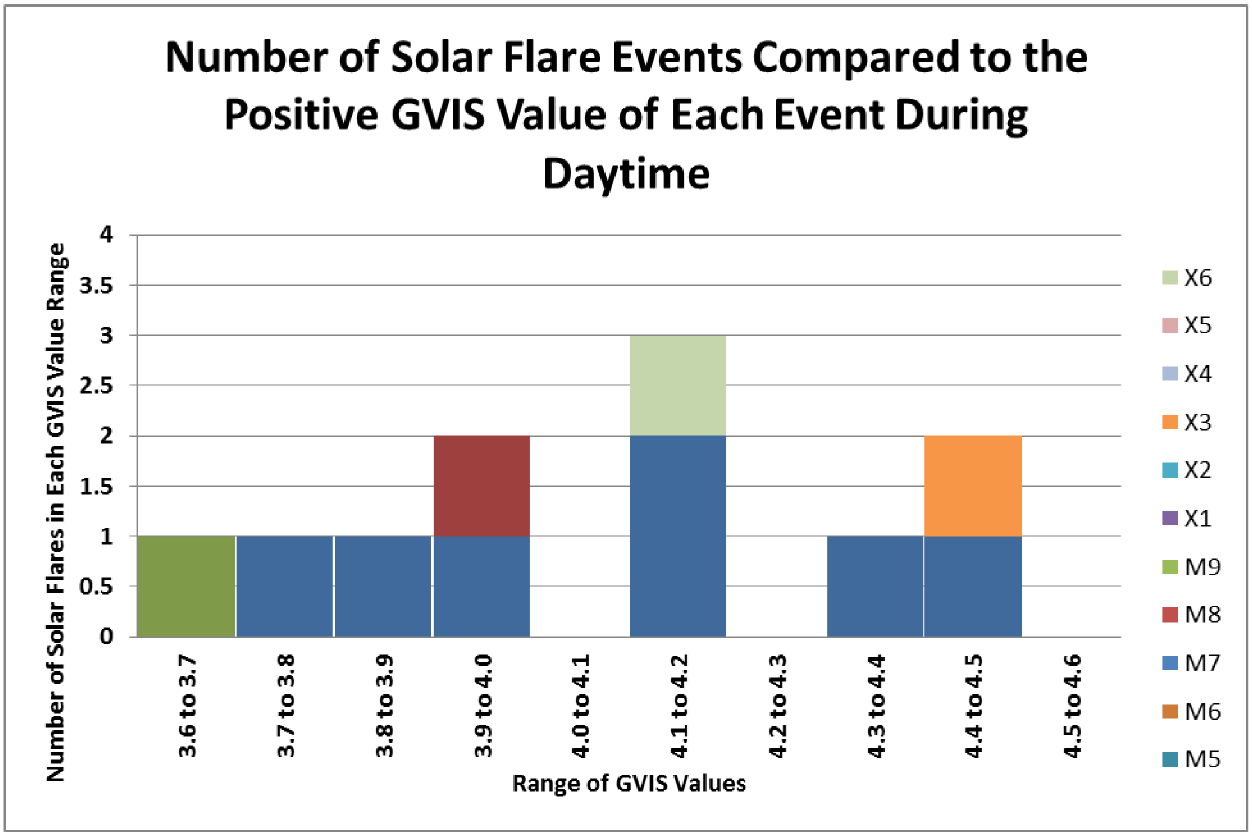

Graph 5

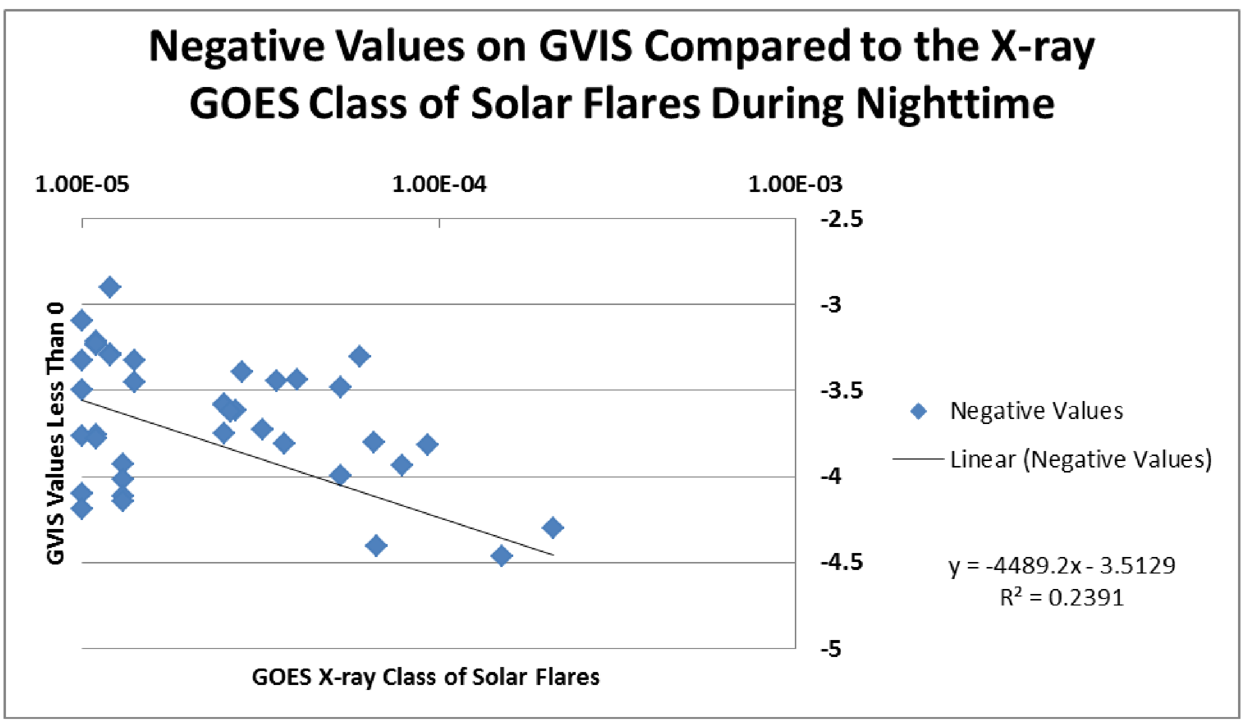

Graph 6

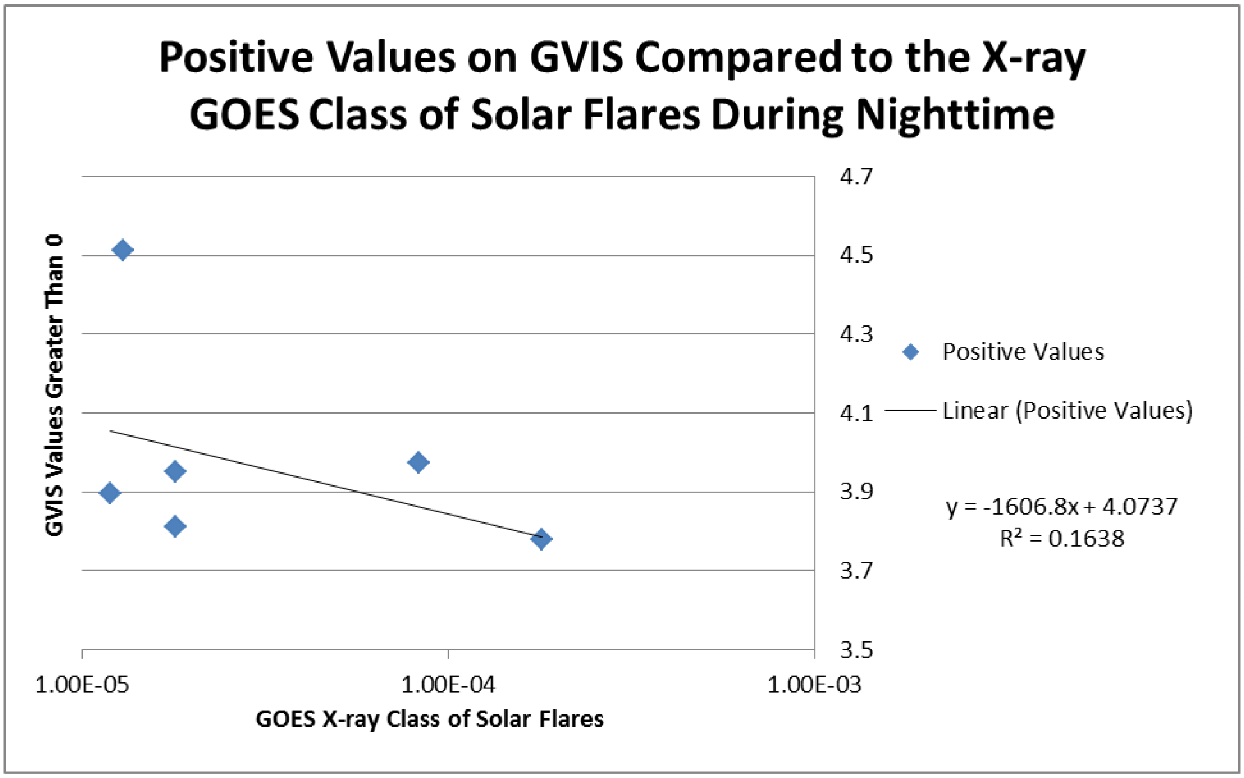

Graph 7

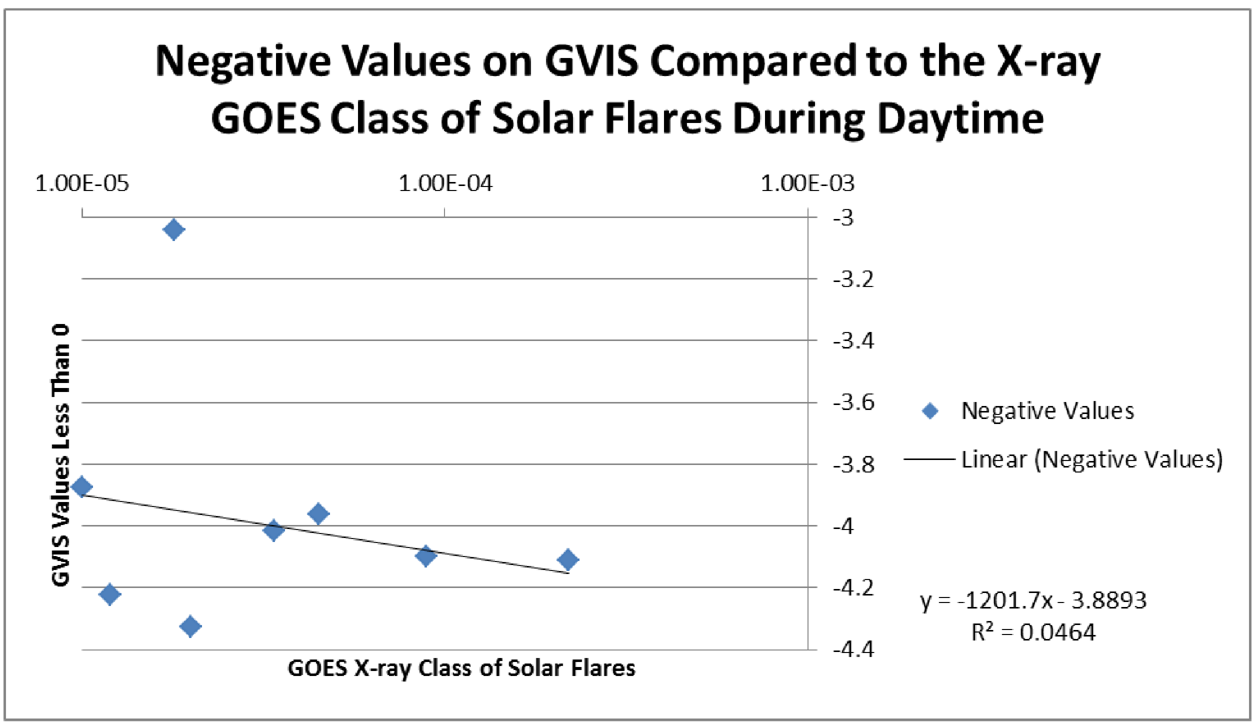

Graph 8

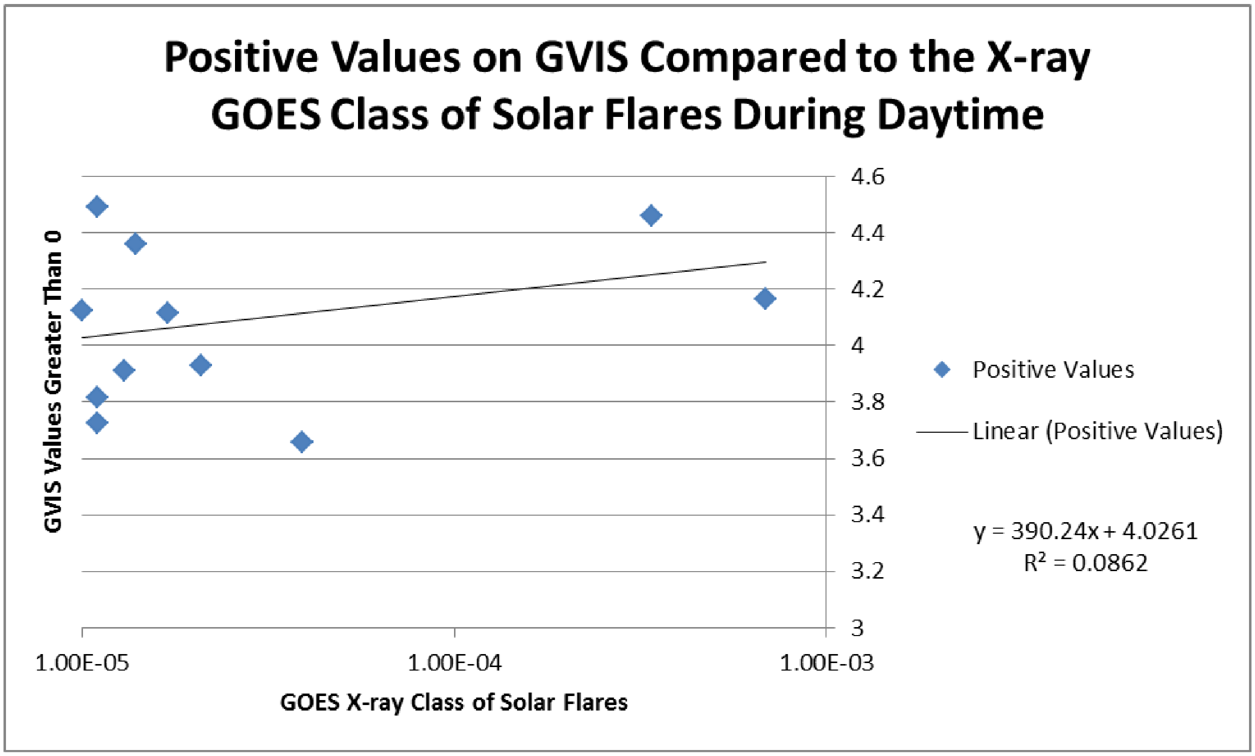

In Table 1, the first column shows the days when solar flares occurred. The second column shows the GOES classifications of the flares in standard GOES form. The third column shows the raw data of the GOES classifications. This data consists of the peak X-ray flux of the flares measured in the wavelength of one to eight Angstroms. The fourth column shows the GVIS value calculated for each flare. Graph 1 is a histogram that shows the distribution of flares classified by GOES among corresponding values of negative GVIS values during night hours. Graph 2 is a histogram that shows the distribution of flares classified by GOES among corresponding values of positive GVIS values during night hours. Graph 3 is a histogram that shows the distribution of flares classified by GOES among corresponding values of negative GVIS values during day hours. Graph 4 is a histogram that shows the distribution of flares classified by GOES among corresponding values of positive GVIS values during day hours. Graph 5 is a scatter plot with a linear trendline that shows the GOES X-ray classification of flares and negative GVIS values during night hours with an R^2 value of 0.2391. Graph 6 is a scatter plot with a linear trendline that shows the GOES X-ray classification of flares and positive GVIS values during night hours with an R^2 value of 0.1638. Graph 7 is a scatter plot with a linear trendline that shows the GOES X-ray classification of flares and negative GVIS values during day hours with an R^2 value of 0.0464. Graph 8 is a scatter plot with a linear trendline that shows the GOES X-ray classification of flares and positive GVIS values during day hours with an R^2 value of 0.0862.

Discussion and Conclusions

Solar flares are events which occur on the Sun that release large amounts of radiation and solar plasma. The GOES classifications of solar flares are classified on an ascending scale based on total X-ray flux in the order of A, B, C, M, and X. Each step of the scale has individual ranks of 1-9 associated with them; M1, M2, M3, for example. In order to measure the effectiveness of solar flaring on the strength of the B_z component of the Earth's magnetic field, a new system was developed. The system was named the GVIS (Geomagnetic Variational Intensity Scale) and measures the intensity of variances in the magnetic field over any amount of time.

In this study, sixty-four solar flare events from 2006 to 2011 were selected for their M or X class status. Solar wind speed, solar wind particle density, and IMF B_z data were downloaded for thirty to seventy-two hours after the release of each flare. Magnetometer data for the B_z component of the Earth's magnetic field was also downloaded for the same time frame as the solar wind and IMF data. Both data sets were used in one hour and five minute average intervals. The magnetometer data was also used in two measurements per second intervals. The solar wind and IMF data was first looked at to find a spike of time when the flares arrived at a point 1.5 million km away from the Earth. Then the magnetometer data was looked at for a two to five hour period of time after the arrival of the flare for effects. Once the general times of effectiveness were found, then a daily graph of the magnetometer data was used to find the GVIS number. The GOES classifications were then graphed on a scatter plot compared against the GVIS values.

As seen in the histogram of Graph 1, M1 flares occur at almost all GVIS value levels, while the stronger flares occur almost uniformly from -3.3 to -4.3 with two X flares occurring at -4.4 to -4.5 during nighttime. Graph 2 shows the same type of result, but with a smaller pool of solar flares to use in the range of positive GVIS values during the nighttime. Graph 3 shows only seven solar flares occurring with a negative GVIS value during the daytime and each flare had a different GVIS value among them. Graph 4 shows a skewed distribution of flares among their GVIS values during the daytime. Graph 5 shows a 0.2391R^2 value between negative GVIS values and their solar flare x-ray flux values during nighttime indicating an extremely weak to no correlation between the two variables. Graph 6 shows a 0.1638 R^2 value between positive GVIS values and their solar flare x-ray flux values during nighttime indicating an extremely weak to no correlation between the two variables. Graph 7 shows a 0.0464 R^2 value between negative GVIS values and their solar flare x-ray flux values during daytime indicating no correlation between the two variables. Graph 8 shows a 0.0862 R^2 value between positive GVIS values and their solar flare x-ray flux values during daytime indicating no correlation between the two variables. ("Correlation coefficient,")

In a previous study (Beach, 2011), the hypothesis that dynamic pressure of solar flares has an effect on the strength of the B_x component of the magnetic field was supported. The higher R^2 value for solar flaring dynamic pressure and the change in the B_x field compared to the lower value for solar wind dynamic pressure and the change in the B_x field indicates this. If flares do affect the Earth's magnetic field, then the strength of the flare as measured by its X-ray flux might correlate with the amount of change it produces in our planet's magnetic field. The B_z field was used in this study in order to better demonstrate the effects of events on the geomagnetic field's strength.

It is also seen in another study that there are GOES classified flares which have X-ray emissions not consistent with their GOES class. The same study indicates that small flares with stronger than usual X-ray emissions tend to fall into one of three different flare models. This suggests that the X-ray flux is not the entire cause for any effects related to the magnetic field. It should be noted, however, that there is only mention of lower GOES class flares in the study along with the models. (Siarkowski, Falewicz & Berlicki) This study is relevant in that it supports the idea of X-ray flux not being the sole variable that affects the geomagnetic field's strength.

A diurnal variation exists in the magnetic field due to ionospheric currents on the dayside of the Earth that disturb the Earth's magnetic field on the dayside throughout the time of the day where the Earth is tilted towards the sun and lessens where the portion of the Earth is tilted away from the sun. This diurnal variation of the Earth's magnetic field is present in events that occurred during the daytime and poses a problem for GVIS calculations due to it being currently near impossible for the diurnal variation to be separated from the effect of solar flares with current technology. The average diurnal variation using seasons from 2006, 2007, 2008, 2010, and 2011 was calculated for the months of July 2006, June 2007, March 2008, June 2010, April 2011, May 2011, June 2011, August 2011, September 2011, October 2011, November 2011, and December 2011. The average diurnal variation between the seasons was 20.41 nT variation per day. A further project to separate the two effects would provide an opportunity for the GVIS to be refined even further. (Svalgaard, 2011)

The 0.2391 R^2 value in Graph 5 shows statistically there is a low correlation between negative GVIS values and GOES class during nighttime. Graph 6 shows a similar statistical approach with an R^2 value of 0.1638 between positive GVIS values and GOES class during nighttime, which is similar to the R^2 value of Graph 5, but is statistically insignificant due to the small number of flare events available for use. The 0.0464 R^2 value in Graph 7 shows statistically that there is no correlation between negative GVIS values and GOES class during daytime, but is statistically insignificant due to the low amount of events that were able to be used. Graph 8 shows a similar statistical approach with an R^2 value of 0.0862 between positive GVIS values and GOES class during daytime, which is similar to the R^2 value of Graph 7, but is also statistically insignificant due to the low amount of events that were able to be used. This study was undertaken to find evidence of whether there was a link between GOES classifications of solar flares and the effect they have on the strength of the magnetic field. The data does not support a correlation between GOES classifications and changes in the strength of the B_z component of the Earth's magnetic field.

With additional data, more flares could be added to the data set to provide a broader range of GOES classification. This would help determine even better if there is or isn’t a correlation. A project investigating the most influential variable of a solar flare on the Earth’s magnetic field would also bring forth a better opportunity to predict the effect of solar flares on the Earth’s magnetic field.

References

Beach, K. (2011, June). *The effect of dynamic pressure on the strength of the earth's magnetic field*. Paper presented at NCSSSMST Student Research Conference. Ncsssmst student research conference.

Correlation coefficient. (n.d.). Retrieved from http://mathbits.com/mathbits/tisection/Statistics2/correlation.htm

Demoulin, P., van Driel-Gesztelyi, L., Schmieder, B., Henoux, J., Csepura, G., & Hagyard, M. (1992). Evidence for magnetic reconnection in solar flares. *SAO/NASA Astrophysics Data System* , 1.

Goes solar x-ray imager. (2010, August 4). Retrieved from http://www.swpc.noaa.gov/sxi/index.html

Lang, K. R. (2006). Sun, Earth and Sky. In K. R. Lang, *Sun, Earth and Sky* (pp. 137-142). New York: Springer Science+Business Media.

Noaa's geostationary and polar-orbiting weather satellites. (2010 February 23). Retrieved from http://noaasis.noaa.gov/NOAASIS/ml/genlsatl.html

NWS internet services team, (2008, Decb 29). *Noaa/nws space weather prediction center*. Retrieved from http://www.swpc.noaa.gov/AboutUs/index.html

Pedersen, L. (2001). Measurements with the proton magnetometer.

Russell, C.T., Chi, P.J., Dearborn, D.J., Ge, Y.S., Kuo-Tiong, B., Means, J.D., Pierce, J.D., Rowe, K.M., and Snare, R.C. (2008). Themis ground-based magnetometers.

Siarkowski, M., Falewicz, R., & Berlicki, A. (2005). Small goes flares with intense hard x-ray emission. Retrieved from http://www.astro.uni.wroc.pl/ludzie/falewicz/www/Prace_files

Smith, C.W. (2011, February 14). *Ace/mag project mag instrument*. Retrieved from http://www.ssg.sr.unh.edu/mag/ace/instrument.html

Space weather prediction center (swpc) historical swpc products and data displays. (2011, Febr   11). Retrieved from http://www.swpc.noaa.gov/ftpdir/warehouse/README

Stone, E.C., Frandsen, A.M., Mewaldt, R.A., Christian, E.R., & Margolies, D. (1998). The advanced composition explorer.

Sun-earth connection. (2011, February 14). Retrieved from http://ds9.ssl.berkeley.edu/themis/mission_sunearth.html

Svalgaard, L. (2011, December 28). Interview by K Beach [Personal Interview].

Swepam solar wind electron proton alpha monitor. (2011, February 14). Retrieved from http://swepam.lanl.gov/

The classification of x-ray solar flares. (n.d.). Retrieved from http://spaceweather.com/glossary/flareclasses.html

Themis overview and goals. (n.d.). Retrieved from http://themis.ssl.berkeley.edu/overview.shtml

Weigel, R. (2005). *Earth's magnetic field*. Retrieved from http://www.bu.edu/cism/cismdx/ref/Labs/2005_AFWA_ShortCourse/Lab03/Lab03